*Pure & Appl. Chem.*, Vol. 47, pp. 147–159. Pergamon Press, 1976. Printed in Great Britain.

# SOME STUDIES ON THE STEREOCHEMISTRY OF CAROTENOIDS†

J. SZABOLCS
Institute of Chemistry, University Medical School, Pécs, Hungary

**Abstract**—The determination of the geometrical configurations of several mono-*cis* carotenoids is reported. The method of combining controlled alkaline permanganate oxidation and $^{13}C$ NMR spectroscopy has provided evidence for the 9-mono-*cis* structure of violeoxanthin and neoxanthin, as well as for the configurational assignments of neozeaxanthin A, neozeaxanthin B, neocapsorubin A, neocapsorubin B and neolutein B.

The stereoisomeric sets of capsanthin and those of lutein epoxide are considered, and several of their new mono-*cis* members are reported. Some configurational assignments based on ultraviolet and light absorption properties are proposed.

An attempt to study the kinetics of *cis–trans* rearrangements in the field of carotenoids was made, and the *cis–trans* isomerism of the lutein epoxide⇌neolutein epoxide A system is commented on.

## INTRODUCTION

In the present paper selected examples of the geometrical isomerism shown by the carbon–carbon double bonds of carotenoids will be discussed. The discussion will be confined to the determination of the configuration of the polyene-chain, to reinvestigation of certain stereoisomeric sets, and to a study of the kinetics of *cis–trans* rearrangement.

## DETERMINATION OF THE GEOMETRICAL CONFIGURATION OF SOME MONO-*CIS*-CAROTENOIDS

The study of the geometrical isomerism of carotenoids was for a long time based on the work done by Zechmeister and his collaborators[1] ($\lambda_{max}$ shift, *cis*-peak effect, i.r. effects, etc.). The total synthesis of certain *cis* carotenoids (Inhoffen, Isler and other workers[1–3]) which enabled an exact study to be made of the physical and chemical properties of the individual *cis* isomers, and also opened up new ways for their comparison, represented an important development. The final solution in the field of structural research into geometrical isomers, which is the most important section of the study of the whole of geometrical isomerism of carotenoids, has recently been brought by the 220–300 MHz PMR and the $^{13}C$ NMR spectroscopical methods.[2–5] $^{13}C$ NMR spectroscopy seems to be particularly promising, and has already been successfully used by several research teams in the structural study of the *cis* isomers of retinal in recent years.[6,7]

In the following I shall describe the use of the recently revived method of oxidative degradation[8] in combination with $^{13}C$ NMR spectroscopy in the study of the geometrical configurations of certain mono-*cis* carotenoids. In the era of $^{13}C$ NMR spectroscopy it seems paradoxical to reintroduce oxidative degradation, which however, in several cases has enabled us to determine the position of the *cis*-double bonds in the polyene chain from 10 mg of material.

### (a) *Oxidative degradation*

Starting with Karrer's classical method [9–11] of alkaline permanganate degradation, we have worked out the conditions for careful, stepwise degradation of 5,6- and 5,8-epoxy carotenoids[8] under which the epoxide end group is preserved. This improved method allowed the isolation of $C_{30}$-, $C_{27}$- and $C_{25}$-epoxy-apo-carotenals, which permitted conclusions as to the structure of the parent carotenoid. The extension of this method to the structural study some mono-*cis* carotenoids such as violeoxanthin, neoxanthin, etc., has already proved useful for configurational assignments. It turned out that in most cases, with mild conditions of oxidation and rapid processing, neither the *cis* starting material, nor the large *cis* epoxy-apo-carotenals obtained underwent stereomutation. Thus from the *cis* or *trans* epoxy-apo-carotenals conclusions were drawn as to the position of the *cis* double bond in the degraded polyene molecule.

In the violeoxanthin molecule for instance there are five possible positions for the *cis* double bond, not excluding the hindered double bonds: 7, 11 (hindered) and 9, 13, 15 (unhindered). As shown in Table 1 the number of *cis* and *trans* $C_{25}$- and $C_{27}$-epoxy-apo-carotenals gives evidence of the exact position of the *cis* double bond in the polyene chain: two *cis* isomers are indicative of 15-*cis* violaxanthin, four *cis* isomers of 13-*cis*-violaxanthin, and one *trans and three cis* isomers of 11-*cis*-violaxanthin. The formation of two *cis* and two *trans* epoxy-apo-carotenals offers no direct evidence concerning the position of the *cis* double bond because both 7-*cis*-violaxanthin and 9-*cis*-violaxanthin may provide four epoxy-apo-carotenals. Despite the hindered character of the double bond in 7-*cis*-violaxanthin, the difference in behaviour between the 7-*cis* and 9-*cis* forms is significant; acid treatment of the 9-*cis*-isomer gave *cis*-auroxanthins while the 7-*cis* isomer would be expected to yield *trans* auroxanthins.

Regarding the structure (Fig. 1) of violaxanthin, oxidative degradation led to two main products, namely *trans* 3-hydroxy - 5,6 - epoxy - 5,6 - dihydro - 10′ - apo - β - caroten - 10′ - al, and its 12′-analogue. The identification of epoxy-apo-aldehydes by their ultraviolet and visible light absorption properties, reduction with $LiAlH_4$, and furanoid oxide tests is demonstrated in Figs. 2 and 3.

A similar experiment with violeoxanthin[12–14] resulted not only in *trans* $C_{25}$- and $C_{27}$-epoxy-apo-aldehydes, but also in their mono-*cis* counterparts. The products could be easily separated by chromatography. Identification of the isomers was carried out in a manner similar to that mentioned before ($\lambda_{max}$, furanoid oxide test, reduction with

†This presentation is based mainly on the doctorial theses of M. Baranyai and P. Molnár. The $^{13}C$ NMR spectra were recorded and interpreted by Dr. L. Radics (Central Research Institute for Chemistry, Budapest).

Table 1. Degradation products used in configurational assignment of violeoxanthin

| Probable location of a *cis* double bond in the violeoxanthin molecule | 5,6-Epoxy-3-hydroxy-5,6-dihydro-10'-apo-β-caroten-10'-al | 5,6-Epoxy-3-hydroxy-5,6-dihydro-12'-apo-β-caroten-12'-al | 5,6-Epoxy-3-hydroxy-5,6-dihydro-10-apo-β-caroten-10-al | 5,6-Epoxy-3-hydroxy-5,6-dihydro-12-apo-β-caroten-12-al | Number of degradation products | |
|---|---|---|---|---|---|---|
| | | | | | All-*trans* form | Monocis form |
| (7 hindered) | 7-*cis* | 7-*cis* | all-*trans* | all-*trans* | 2 | 2 |
| 9 | 9-*cis* | 9-*cis* | all-*trans* | all-*trans* | 2 | 2 |
| (11 hindered) | 11-*cis* | 11-*cis* | 11-*cis* | all-*trans* | 1 | 3 |
| 13 | 13-*cis* | 13-*cis* | 13-*cis* | 13-*cis* | 0 | 4 |
| 15 | 15(15')-*cis* | 15(15')-*cis* | 15(15')-*cis* | 15(15')-*cis* | 0 | 2 |

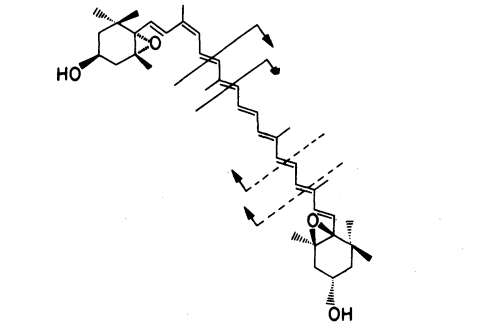


Fig. 1. Cleavage of violeoxanthin and violaxanthin.

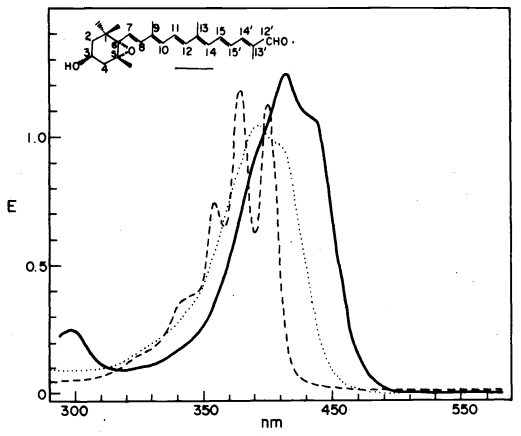


Fig. 2. Ultraviolet and visible light absorption spectra of 5,6-epoxy-3-hydroxy-5,6-dihydro-10'-apo-β-caroten-10'-al (——), 5,6-epoxy-3-hydroxy-5,6-dihydro-10'-apo-β-caroten-10'-ol (- - - -), and 5,8-epoxy-3-hydroxy-5,8-dihydro-10'-apo-β-caroten-10'-al (s) (·····), (in benzene).

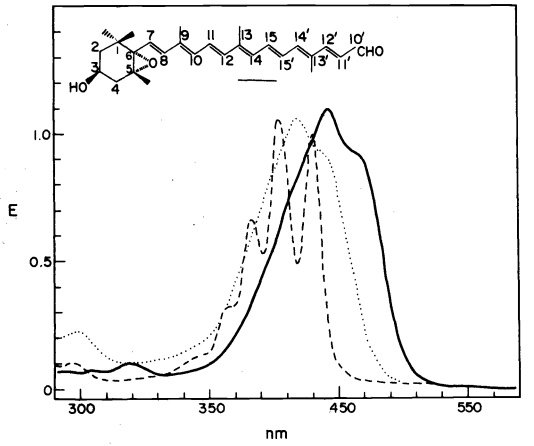


Fig. 3. Ultraviolet and visible light absorption spectra of 5,6-epoxy-3-hydroxy-5,6-dihydro-12'-apo-β-caroten-12'-al (——), 5,6-epoxy-3-hydroxy-5,6-dihydro-12'-apo-β-caroten-12'-ol (----) and 5,8-epoxy-3-hydroxy-5,8-dihydro-12'-apo-β-caroten-12'-al(s) (·····) (in benzene).

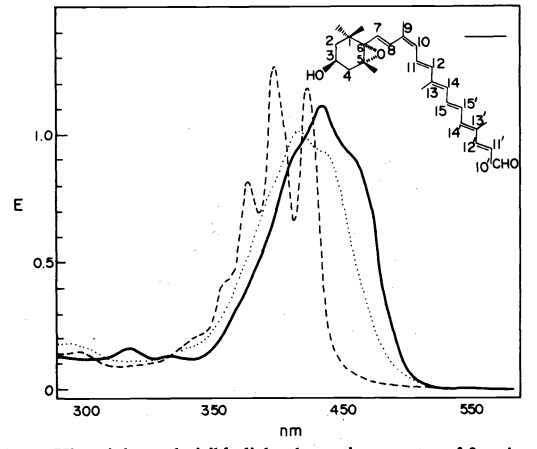


Fig. 4. Ultraviolet and visible light absorption spectra of 9-*cis*-5,6-epoxy-3-hydroxy-5,6-dihydro-10'-apo-β-caroten-10'-al (——), 9-*cis*-5,6-epoxy-3-hydroxy-5,6-dihydro-10'-apo-β-caroten-10'-ol (----) and 9-*cis*-5,8-epoxy-3-hydroxy-5,8-dihydro-10'-apo-β-caroten-10'-al(s) (·····) (in benzene).

$LiAlH_4$, etc.) (Figs. 4 and 5), however, in addition the *cis* isomers were converted into the corresponding *trans* analogues by iodine isomerisation.

When neoxanthin X[15,16] was subjected to degradation, only *trans* $C_{27}$- and $C_{25}$-epoxy-apo-aldehydes appeared, which confirmed the all-*trans* geometrical structure of neoxanthin X (Fig. 6). On the other hand, from neoxanthin only *cis* $C_{27}$-, $C_{25}$-epoxy-apo-aldehydes formed. So it must

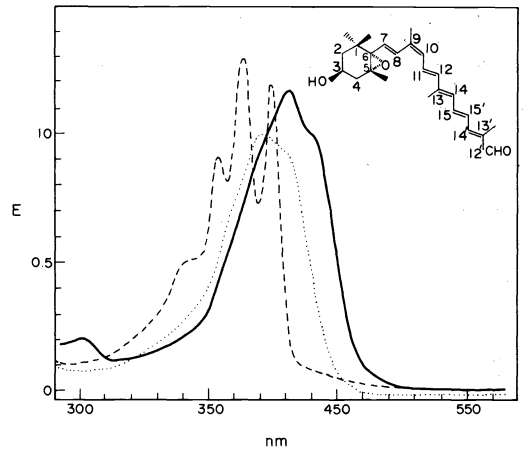


Fig. 5. Ultraviolet and visible light absorption spectra of 9 - *cis* - 5,6 - epoxy - 3 - hydroxy - 5,6 - dihydro - 12′ - apo - β - caroten - 12′ - al (——), 9 - *cis* - 5,6 - epoxy - 3 - hydroxy - 5,6 - dihydro - 12′ - apo - β - caroten - 12′ - ol (----) and 9 - *cis* - 5,8 - epoxy - 3 - hydroxy - 5,8 - dihydro - 12′ - apo - β - caroten - 12′ - al(s) (·····) (in benzene).

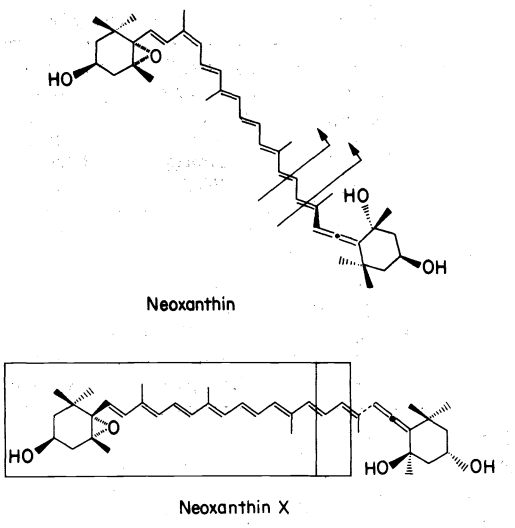


Fig. 6. Cleavage of neoxanthin X and neoxanthin.

be concluded that neoxanthin and violeoxanthin with a *cis* double bond have a 9-mono-*cis* geometrical configuration, and violaxanthin and neoxanthin have an all-*trans* character (Table 2).

The data in Table 3 show that the epoxy-apo-aldehydes obtained by the oxidation of violeoxanthin and neoxanthin are indeed *cis* fragments since the i.r. absorption maxima of their furamoid oxides compared with those of the all-*trans* analogues are shifted about 2 nm towards the shorter wavelengths. In Table 3 the light absorption properties of the degradation products and their derivatives are also presented for comparison. The 3 - hydroxy - 5,6 - epoxy - 5,6 - dihydro - 10′ - apo - β - caroten - 10′ - al (molecular ion *m/e*: 408; fragments: *m/e* 221, *m/e* 181, M-18, M-28, M-92) and 3 - hydroxy - 5,6 - epoxy - 5,6 - dihydro - 12′ - apo - β - caroten - 12′ - al (molecular ion *m/e*: 382; fragments: *m/e* 221, M-18, M-29, M-95), most important for the identification of the different epoxy-apo-aldehydes, were prepared in crystalline state by degradation of natural violaxanthin diacetate, The key reactions in

Table 2. Degradation products of some mono-*cis* and all-*trans* carotenoids

| | 5,6-Epoxy-3-hydroxy-5,6-dihydro-10′-apo-β-caroten-10′-al | 5,6-Epoxy-3-hydroxy-5,6-dihydro-12′-apo-β-caroten-12′-al | 5,6-Epoxy-3-hydroxy-5,6-dihydro-10-apo-β-caroten-10-al | 5,6-Epoxy-3-hydroxy-5,6-dihydro-12-apo-β-caroten-12-al | Number of degradation products | |
|---|---|---|---|---|---|---|
| | | | | | All-*trans* form | Mono-*cis* form |
| Violaxanthin | all-*trans* | all-*trans* | all-*trans* | all-*trans* | 2 | |
| Violeoxanthin | all-*trans* | all-*trans* | mono-*cis* | mono-*cis* | 2 | 2 |
| Neoxanthin | mono-*cis* | mono-*cis* | | | | 2 |
| Neoxanthin X | all-*trans* | all-*trans* | | | 2 | |

Table 3. Spectral data of the degradation products obtained by the oxidation of violeoxanthin diacetate

| Oxidation products† of violeoxanthin diacetate | $\lambda_{max}$ in benzene | $\lambda_{max}$ in HCl-benzene | $\lambda_{max}$ after $LiAlH_4$ treatment in benzene | $\lambda_{max}$ after $LiAlH_4$ treatment in HCl-benzene |
|---|---|---|---|---|
| *cis*-5,6-epoxy-3-hydroxy- | (468) | 437 | 424 | 403 |
| 5,6-dihydro-10′-apo-β- | 439 | 415 | 398 | 380 |
| caroten-10′-al | | | 377 | 361 |
| *cis*-5,6-epoxy-3-hydroxy- | (434) | (410) | 397 | 372 |
| 5,6-dihydro-12′-apo-β- | 410 | 390 | 375 | 353 |
| caroten-12′-al | | | 356 | 337 |
| *trans*-5,6-epoxy-3-hydroxy- | (470) | (442) | 428 | 405 |
| 5,6-dihydro-10′-apo-β- | 442 | 419 | 402 | 381 |
| caroten-10′-al | | | 381 | 362 |
| *trans*-5,6-epoxy-3-hydroxy- | (440) | (412) | 400 | 373 |
| 5,6-dihydro-12′-apo-β- | 414 | 392 | 377 | 353 |
| caroten-12′-al | | | 358 | 339 |

†In the sequence of decreasing absorption affinities.

the structure determination of $C_{25}$- and $C_{27}$-epoxy-apo-aldehydes are shown in Fig. 7.

Incidentally, it should be mentioned that apo-10'-violaxanthal isolated by Curl[17] from Valencia-orange was doubtlessly a 9-mono-*cis* isomer of 3 - hydroxy - 5,6 - epoxy - 5,6 - dihydro - 10' - apo - $\beta$ - caroten - 10' - al and not its *trans* form as has often been stated[8] since. This assumption is supported by the visible light absorption of 9-mono-*cis* - 3 - hydroxy - 5,6 - epoxy - 5,6 - dihydro - 10' - apo - $\beta$ - caroten - 10' - al, which agrees with Curl's finding.

Furthermore, the method oxidative degradation, has recently been successfully used for determining the position of the *cis* double bond in the neolutein B molecule (Fig. 8). It was assumed by Zechmeister and A. Polgár[18] that neolutein B was the 9- or 9'-mono-*cis* form of lutein (low *cis*-peak and $\lambda_{max}$ shift). Oxidation of neolutein B by alkaline permanganate unambiguously led to the 9-mono-*cis* structure. As is shown in Table 4 both the different $\alpha$-, and $\beta$-apo-aldehydes obtained from the oxidation of lutein have all-*trans* structure. However, among the oxidation products of neolutein B the 3 - hydroxy - 10' - apo - $\beta$ - caroten - 10' - al and the 3 - hydroxy - 12' - apo - $\beta$ - caroten - 12' - al appear exclusively in *cis* form. Since $\alpha$-apo-aldehydes are *trans* and $\beta$-apo-aldehydes are *cis* in the case of oxidation of neolutein B it is obvious that neolutein B has 9-mono-*cis* structure. Analyses of the different apo-aldehydes was based on visible light absorption data, mixed-chromatogramms, reversible isomeric tests, etc.

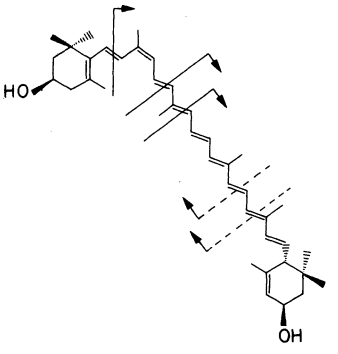


Fig. 8. Cleavage of neolutein B and lutein.

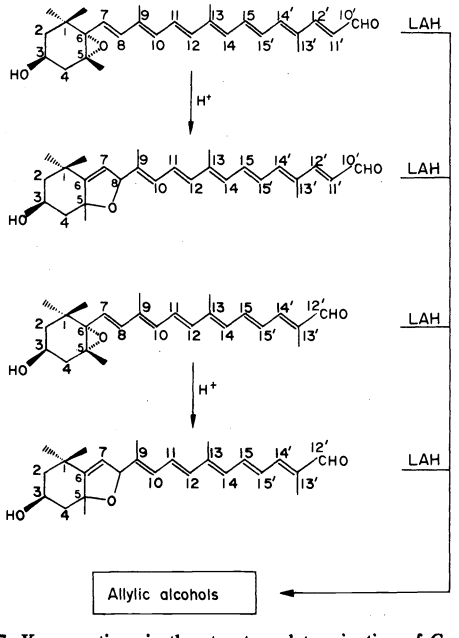


Fig. 7. Key reactions in the structure determination of $C_{25}$- and $C_{27}$-epoxy-apo-aldehydes.

It should be mentioned that the degradation method when applied to neolutein A proved to be a failure because of the great number of *cis* and *trans* fragments resulting from conversion of neolutein A into lutein during the oxidation procedure. In conclusion it can be said that we have succeeded in determining and proving the geometrical structures of violeoxanthin, neoxanthin, neoxanthin X and neolutein B by means of oxidative degradation under controlled conditions. Finally, we are planning to apply our method to investigation of the geometrical configuration of mono-*cis* furanoid oxides, too.

(b) *Carbon*-13 *magnetic resonance spectroscopy*

We shall now consider the application of $^{13}C$ NMR spectroscopy to the determination of the geometrical configuration of some mono-*cis* carotenoids. We started our studies with zeaxanthin and capsorubin (symmetrical types), whose mono-*cis* isomers are reported in the

Table 4. Oxidation products of lutein and neo-lutein B

| Oxidation products | | Starting material: Lutein | Starting material: Neo-lutein-B | $\lambda_{max}$ in hexane | | | $\lambda_{max}$ after $LiAlH_4$ treatment in hexane | | |
|---|---|---|---|---|---|---|---|---|---|
| 3'-hydroxy-8-apo- | *trans* | + | (+)† | 477 | 448 | 425 | 443 | 416 | 393 |
| $\alpha$-caroten-8-al | *cis* | – | (+)† | 471 | 443 | 422 | 440 | 413 | 390 |
| 3'-hydroxy-10-apo- | *trans* | + | + | 452 | 425 | 404 | 417 | 391 | 371 |
| $\alpha$-caroten-10-al | *cis* | – | – | | | | | | |
| 3'-hydroxy-12-apo- | *trans* | + | + | 426 | 403 | (382) | 389 | 367 | 350 |
| $\alpha$-caroten-12-al | *cis* | – | – | | | | | | |
| 3-hydroxy-10'-apo- | *trans* | + | – | (458) | 433 | | 419 | 396 | 376 |
| $\beta$-caroten-10'-al | *cis* | – | + | (452) | 427 | | 415 | 393 | 373 |
| 3-hydroxy-12'-apo- | *trans* | + | – | (428) | 408 | | 390 | 372 | (354) |
| $\beta$-caroten-12'-al | *cis* | – | + | (425) | 404 | | 386 | 368 | (350) |

†Ratio of the *cis* and *trans* isomers $\cong$ 5:1.

literature. The spatial structure of their neo A and that of their neo B forms were tentatively assigned by Zechmeister and his co-workers; neozeaxanthin A and neocapsorubin A with high *cis*-peaks represent 13-*cis* isomers, while neozeaxanthin B and neocapsorubin B with low *cis*-peaks represent 9-*cis* isomers (Figs. 9, 10). (The 9- and 13-*cis* isomers of zeaxanthin and capsorubin were prepared by stereomutation of the corresponding all-*trans* carotenoids in our laboratory.) The correctness of the above stereochemical conclusions was conclusively demonstrated by a carbon-13 NMR study.

The high sensitivity of carbon chemical shifts on changes in steric environment renders $^{13}C$ NMR spectroscopy a valuable analytical aid in distinguishing stereoisomeric structures. Recent studies on retinal isomers and related model compounds,[6,7] as already mentioned, provided promising prospects for the c.m.r. approach in the carotenoid field. Two major conclusions of the earlier studies[6,7,19] seem to apply in most practical cases:

*First*: In the all-*trans* isomers, the $sp^2$ carbon resonances of the polyenic framework follow a more-or-less regular pattern. A typical example is furnished by the partial spectrum of the all-*trans* zeaxanthin shown on Fig.

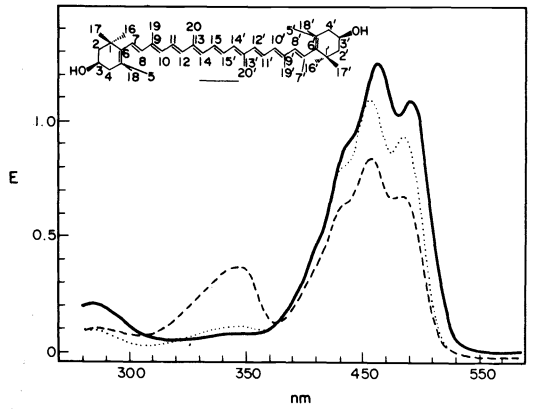


Fig. 9. Ultraviolet and visible light absorption spectra of zeaxanthin (——), neo-zeaxanthin A (----) and neo-zeaxanthin B (·····) (in benzene).

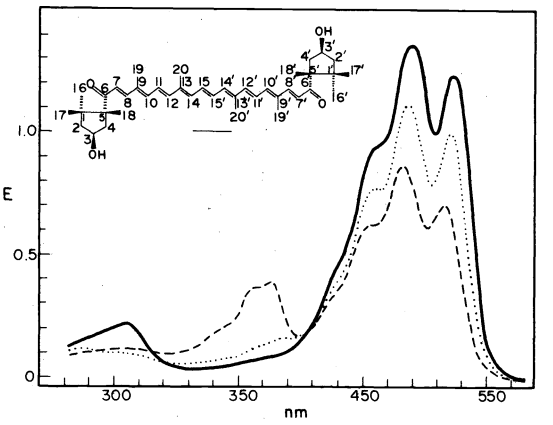


Fig. 10. Ultraviolet and visible light absorption spectra of all-*trans*-capsorubin (——), neo-capsorubin A (----) and neo-capsorubin B (·····) (in benzene).

11, where the individual resonances closely follow the pattern observed for $\beta$-carotene: carbons 7 and 11 appear as the most shielded, 8, 12, 9 and 13 the least shielded nuclei, while resonances due to carbons 14, 10 and 15 show up in the mid-range. Conjugated electron-withdrawing (or-donating) end-groups may change this pattern *via* alternating polarization of the polyenic system; the polarizing effect is attenuated with increasing number of intervening bonds. By taking advantage of the regularity of the polarizing effect of the carbonyl end group, assignment of the individual $sp^2$ resonances in the spectrum of the all-*trans* capsorubin was straightforward. The altered sequence of lines is seen on the right hand side spectrum of Fig. 11.

The *second* important finding of former studies indicate that the occurrence of a *cis* double bond in the polyenic chain gives rise to well-defined isomerization shifts in the resonances of carbons situated at and near the isomerization site. In accord with the so-called gamma-effect operating through the mutual polarization of sterically interacting C–H bondings, carbons whose steric compression is relieved by isomerization are shifted downfield (←) (positive shift), while carbons experiencing higher steric

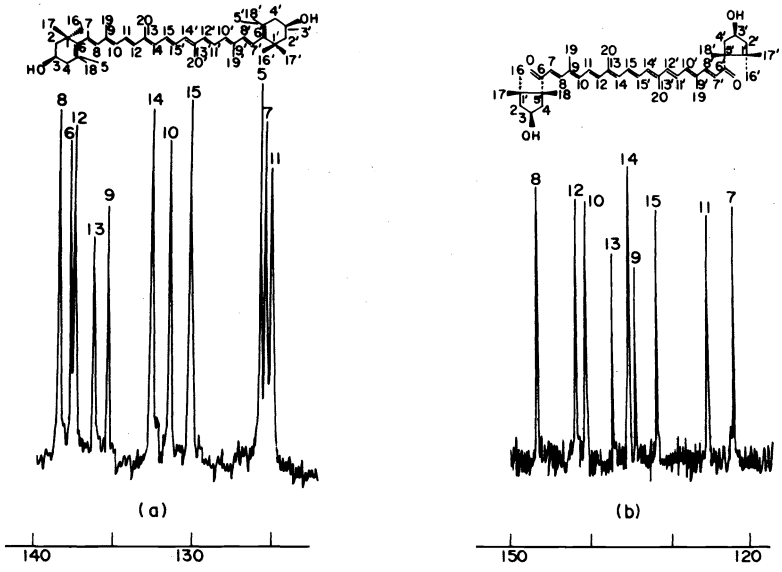


Fig. 11. $^{13}C$ NMR spectra ($sp^2$ range) of zeaxanthin (a) and capsorubin (b).

crowding in the *cis* form have their resonances shifted upfield (→) (negative shift). This is illustrated on Fig. 12 showing the partial spectrum of neozeaxanthin B. The resonances of the *trans* end carbons remain practically unaffected by isomerization while the *cis* end carbon resonances (denoted by primed numbers) exhibit shifts typical of the 9-*cis* configuration. Since the magnitude and sign of these steric shifts are highly specific as to the site of isomerization, even an incomplete assignment of the spectrum may serve as a firm basis for the stereochemical conclusion. Here, for instance, the occurrence of a resonance doubling of carbons 5 and 6 alone is sufficient to locate the isomerization near the end-group, i.e. at position 9. A comparison of the complete spectra of capsorubin with that of neocapsorubin B, seen on Fig. 13, gives another example on how partial interpretation can be used for the location of the *cis* double bond. (For clarity, the spectrum of the *cis* isomer, shown on the upper trace, is expanded horizontally.) The appearance of a methyl resonance, C-9 Me or C-13 Me, shifted downfield by about 8 ppm generally indicate 9 or 13-*cis* bonding, respectively. Minor splittings of some $sp^3$ resonances (carbons 1, 5 and C-5 Me) along with a somewhat larger shift of the C-6 carbonyl signal, however, suggest that the *cis* bonding is at position 9.

By similar reasoning, assignment of the spectra of neozeaxanthin A and neocapsorubin A permitted the location of the *cis* double bond at position 13 in both cases. The observed steric shifts of the *cis* end resonances relative to the *trans* end values are shown diagrammatically on Fig. 14.

Presently we are extending our carbon-13 NMR studies to carotenoids with two different end groups, and to derivatives with more than one *cis* double bonds.

(Experimental. Natural abundance $^{13}C$ NMR spectra were obtained at 25.16 MHz using a Varian XL-100-15 spectrometer equipped with a Varian Fourier transform accessory and 620 L computer. The samples were prepared as 0.04–0.05 M solutions in $CDCl_3$ with tetramethylsilane as the internal reference. The probe temperature was maintained at 32°C.)

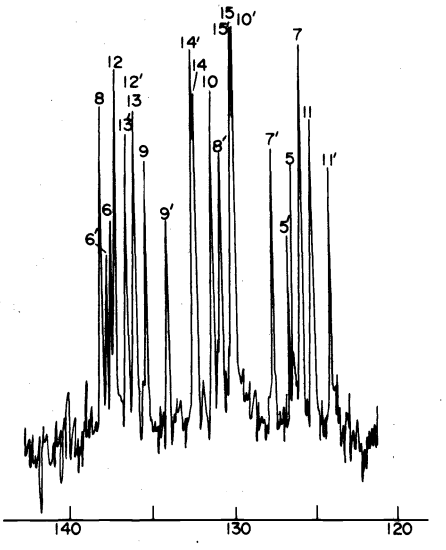


Fig. 12. $^{13}C$ NMR spectrum of neozeaxanthin B $sp^2$ range.

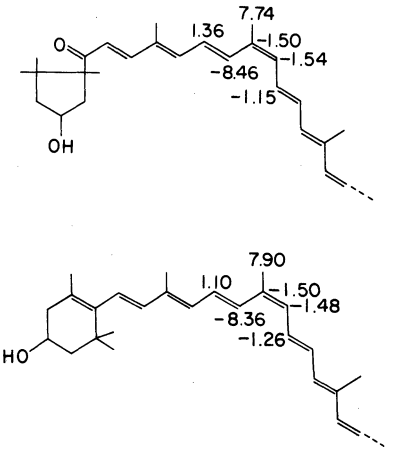


Fig. 14. Steric shifts for neozeaxanthin A and neocapsorubin A.

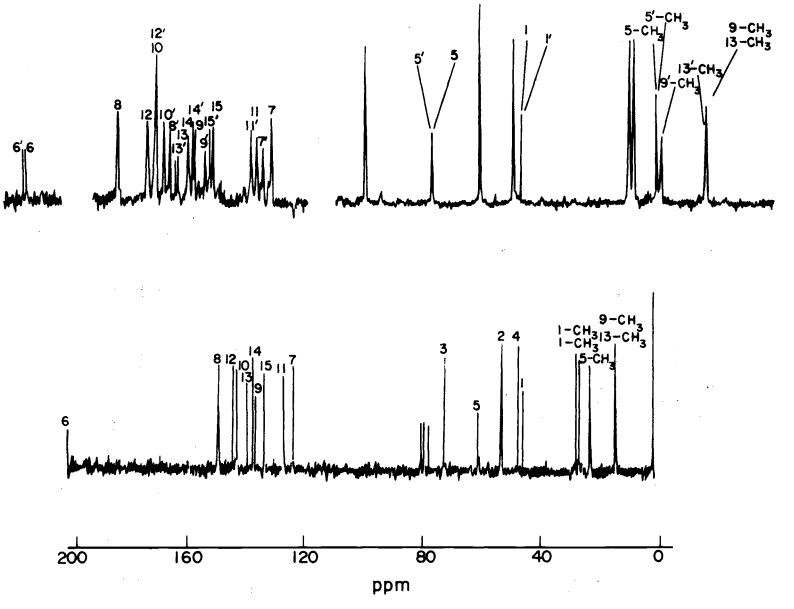


Fig. 13. $^{13}C$ NMR spectra of capsorubin and neocapsorubin B (horizontally expanded).

## REINVESTIGATION OF CERTAIN STEREOISOMERIC SETS

At present, there is a gap between the number of calculated and observed geometrical forms of mono-*cis* carotenoids. As is well known, for instance zeaxanthin and capsorubin (symmetrical types) can be converted into their 9-*cis* and 13-*cis* spatial forms by iodine catalysis.[19,20,21] In view of the hindered bonds[1,22] and the finding, well known in the literature, that central-mono-*cis* forms[23] usually do not appear in the equilibrium mixture of isomers the appearance of two mono-*cis* isomers of zeaxanthin and two of capsorubin had been expected a priori. However, capsanthin (unsymmetrical type), whose molecule structure is half capsorubin and half zeaxanthin, gives only two[24] instead of four mono-*cis* isomers under the same conditions. Theoretically, the spatial forms 9-, 9′-, 13- and 13′- had been expected as stabile isomers. Although the difference in thermodynamic behaviour between the four isomers and other contributing factors might exclude the appearance of all four mono-*cis* capsanthins we made an attempt chromatographically to separate also the two "missing" mono-*cis* isomers from the equilibrium mixture of capsanthin. It was therefore interesting to carry out systematic studies in the field just discussed.

### *Capsanthin set*

When treated with iodine, capsanthin yielded two mono-*cis* isomers: neo A and neo B[24]. Considering the respective $\lambda_{max}$ shifts and *cis*-peak intensities it was assumed[1,25] that the *cis* double bond of the neo A form must be located in a more central position than that of the neo B form.

During subsequent experiments on the chromatographic separation of the equilibrium mixture of capsanthin we succeeded in isolating four mono-*cis* capsanthins, i.e. the two known and the two "missing" mono-*cis* isomers. A sample of neocapsanthin A on calcium carbonate column yielded two red zones, and the neo form A adsorbed above the neo form A* according to our nomenclature. Similarly, neocapsanthin B resulted in two individual isomers, the neo B isomer adsorbed above the neo B* isomer.

Figure 15 shows that the neo forms A and A* have high *cis*-peaks of the same intensity ($Q = 1.7$), but the wavelength difference, in nm, between $\lambda_{max}$ of all-*trans* capsanthin and those of the two *cis* isomers is not at all the same (4 and 8 nm, respectively). Considering that capsanthin and the neocapsanthins exhibit no sharp $\lambda_{max}$ at 520 nm, we use the $\lambda_{max}$ shifts at 486 nm in benzene solution. The ultraviolet and light absorption curves of the neo forms B and B$^x$ which are presented in Fig. 16 exhibit low *cis*-peaks and different $\lambda_{max}$ shifts (4 nm for neo B and 7 nm for neo B*).

As seen from Table 5 comparison of the $\lambda_{max}$ shifts and *cis*-peak values of neocapsorubins and neozeaxanthins

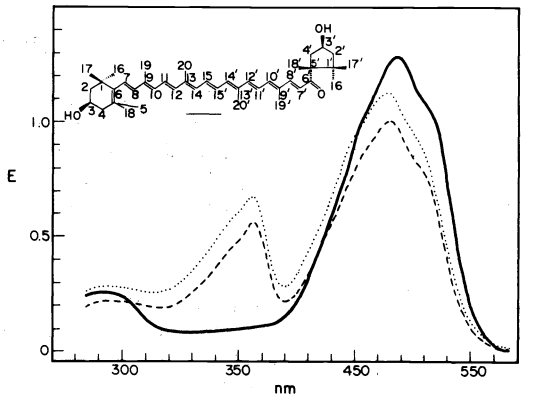


Fig. 15. Ultraviolet and visible light absorption spectra of all-*trans*-capsanthin (——), neo-capsanthin A (----) and neo-capsanthin A* (·····) (in benzene).

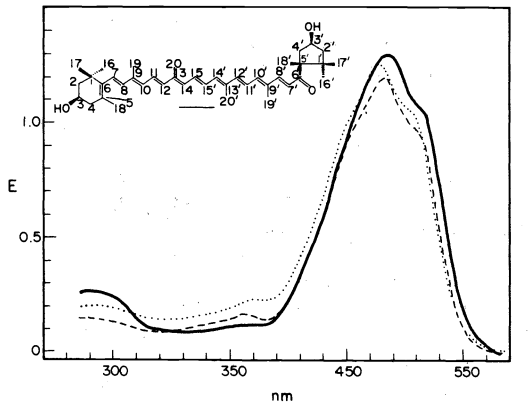


Fig. 16. Ultraviolet and visible light absorption spectra of all-*trans*-capsanthin (——), neo-capsanthin B (----) and neo-capsanthin B* (·····) (in benzene).

with those of neocapsanthins all of which have one end group of zeaxanthin and one end group of capsorubin, led to the conclusion that the $\lambda_{max}$ shifts and *cis*-peaks of neocapsanthins are, at first sight, additive. In detail, putting together one half of the neocapsorubin A and one half of the all-*trans* zeaxanthin gives neocapsanthin A, and one half of the all-*trans* capsorubin and one half of the neozeaxanthin A gives neocapsanthin A*. Similarly, neocapsorubin B can be built up formally from one half of the neocapsorubin B and one half of the all-*trans* zeaxanthin, and neocapsorubin B* from one half of the all-*trans* capsorubin and one half of the neozeaxanthin B.

Since the geometrical structure of neozeaxanthin A and B, as well as the geometrical structure of neocapsorubin A and B had just been solved by $^{13}$C NMR spectroscopy, it was tentatively concluded (Fig. 17), that neocapsanthin A was the 13′-*cis*, neocapsanthin A* the 13-*cis*, neocapsan-

Table 5. Spectral data of mono-*cis* capsanthins and related mono-*cis* carotenoids

| | Mono-*cis* capsorubins | | Mono-*cis* zeaxanthins | | Mono-*cis* capsanthins | | | |
|---|---|---|---|---|---|---|---|---|
| | neo A (13-*cis*) | neo B (9-*cis*) | neo A (13-*cis*) | neo B (9-*cis*) | neo A (13′-*cis*) | neo A* (13-*cis*) | neo B (9′-*cis*) | neo B* (9-*cis*) |
| λ-shift at $E_{max}$ (nm) | 7 | 4 | 10 | 8 | 7 | 10 | 4 | 8 |

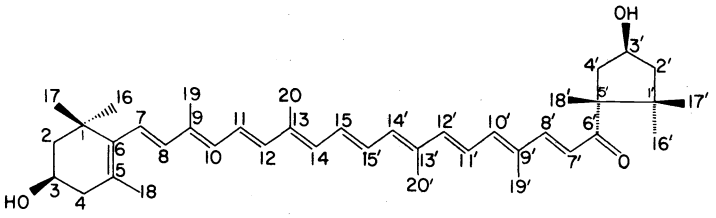

Fig. 17. Capsanthin.

thin B the 9′-*cis*, and neocapsanthin B* the 9-*cis* spatial forms. The symbolic spatial structure of the four neocapsanthins is illustrated in Fig. 18.

To check the additivity and the spectral effect of the distance from the *cis* double bond of the carbonyl group present in the chromophore, the four mono-*cis* neocapsanthins were reduced with $NaBH_4$.[26] Neocapsanthin A and A* provided neocapsanthols with the same high *cis*-peak and the same $\lambda_{max}$ (Fig. 19). In agreement with this observation neocapsanthin B and B* gave neocapsanthols also with the same low *cis*-peak and the same $\lambda_{max}$ (Fig. 20).

*Lutein epoxide set*

Unlike capsanthin, this structurally unsymmetrical carotenoid contains a symmetrical chromophore system with nine conjugated double bonds (Fig. 21). In the case lutein epoxide, four mono-*cis* isomers (excluding the central form) were expected upon iodine catalyses. Actually, only two main isomers were observed,[19] viz. neotaraxanthin A and neotaraxanthin B. (It will be noted that naturally occuring "tareoxanthin"[27] is a mixture of neotaraxanthin A, B and a small amount of *cis*-violaxanthin.) As is well known from the literature,[28–30] taraxanthin has often been confused with native lutein epoxide, which means all data on taraxanthin only apply to native lutein epoxide. Thus there are two mono-*cis*

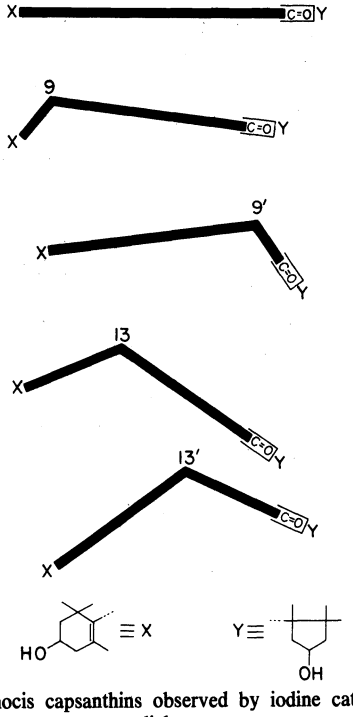

Fig. 18. Monocis capsanthins observed by iodine catalysis, in light.

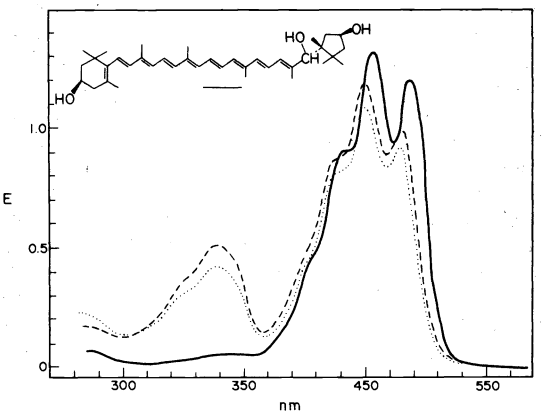

Fig. 19. Ultraviolet and visible light absorption spectra of all-*trans*-capsanthol (——), neo-capsanthol A (----) and neo-capsanthol A* (·····) (in benzene).

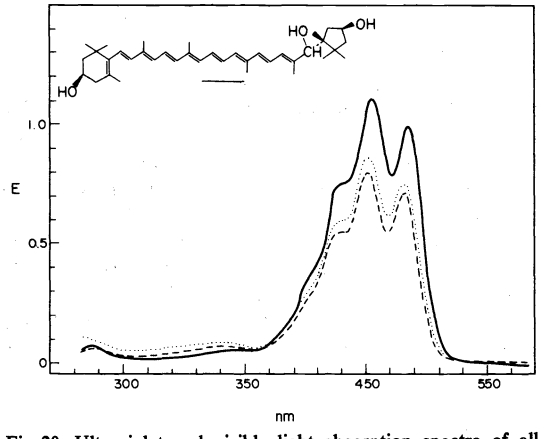

Fig. 20. Ultraviolet and visible light absorption spectra of all-*trans*-capsanthol (——), neo-capsanthol B (----) and neo-capsanthol B* (·····) (in benzene).

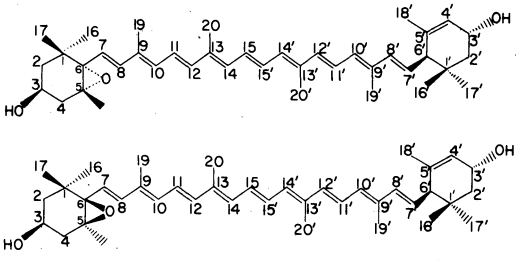

Fig. 21. Native (anti) and semi-synthetic (syn) lutein epoxides.

isomers[31] of lutein epoxide, neo A ($\lambda_{max}$ shift 5 nm) with a high *cis*-peak ($Q = 1.7$), and the neo B form ($\lambda_{max}$ shift 3 nm) almost without a *cis*-peak. Evidently, neolutein epoxide B represents a peripheral mono-*cis* form (9 or 9′),

and the *cis* double bond occupies a more central position (13 or 13′) in neolutein epoxide A.

Searching for the two "missing" mono-*cis* neolutein epoxides, we treated native lutein epoxide with iodine in the usual manner[1] in order to obtain neolutein epoxide A and B. After isolation of the neo A and neo B forms they were subjected to systematic chromatography, which finally resulted in the zone of neolutein epoxide A and also that of B splitting on the chromatographic column into two individual isomers: neo A, neo A*, and neo B, neo B* forms, respectively. (The asterisks indicate weaker absorption affinities.)

As seen from Fig. 22, neo A and A* exhibit the same u.v.-light absorption properties ($Q = 2.0$; $\lambda_{max}$ shift = 7 nm). The epoxide-furanoid rearrangement of the neo A and neo A* forms causes the same hypsochromic shift leaving the high *cis*-peak unaffected (Fig. 24). The ratio of the steric forms obtained by stereomutation is about 1:1. It should be noted that in boiling benzene solution of lutein epoxide, both neo A and neo A* isomers appear. These similarities were taken to indicate that the neo A and neo A* forms represent 13-, and 13′-mono-*cis*-lutein epoxide, respectively, and are strong evidence against the existence of a middle *cis* form.

As Fig. 23 shows neolutein epoxide B and B* also exhibit the same u.v.-visible spectral curves ($\lambda_{max}$ shift 4 nm), which are almost flat in the *cis*-peak region. On treatment with dilute acid, both isomers convert into furanoid oxides with the same hypsochromic shift (Fig. 24). The amounts of neo B and neo B* in the equilibrium mixture after iodine catalysis are about equal. A significant difference between the neo A (A*) and neo B (B*) isomers, however, is that the neo B(B*) isomers do not form in a refluxed benzene solution of lutein epoxide. This may be caused by the bulky end groups which, in some way, sterically hinder conversion of the double bond in the peripheral 9 or 9′ position. It was therefore concluded that the neo B and neo B$^x$ forms represent 9- or 9′-mono-*cis*-lutein epoxide (Fig. 25). However, we can not yet assign exact spatial structure to neo A and A* or B and B* within the isomeric pairs.

As had been expected a similar examination of

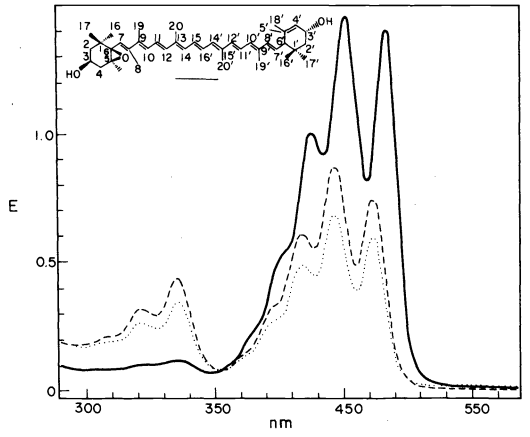


Fig. 22. Ultraviolet and visible light absorption spectra of syn-lutein epoxide (——), syn-neo-lutein epoxide A (----) and syn-neo-lutein epoxide A* (·····) (in benzene).

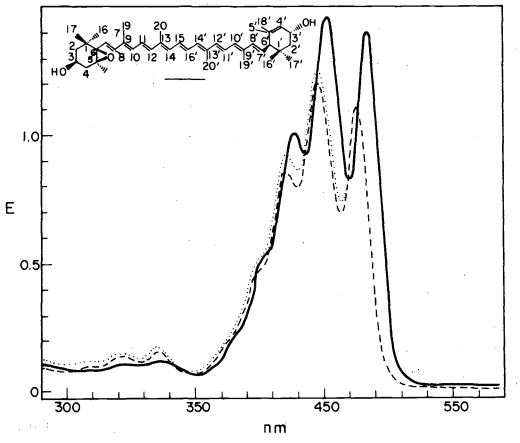


Fig. 23. Ultraviolet and visible light absorption spectra of syn-lutein epoxide (——), syn-neo-lutein epoxide B (----) and syn-neo-lutein epoxide B* (·····) (in benzene).

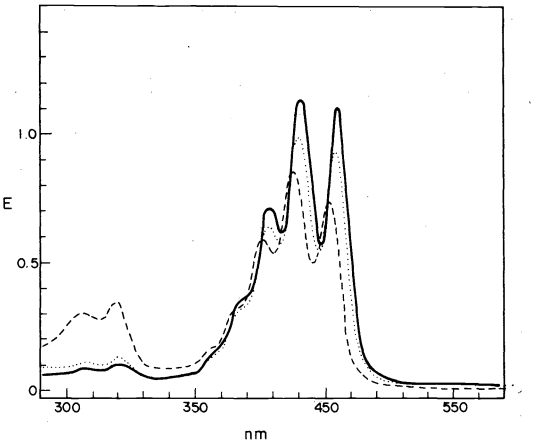


Fig. 24. Ultraviolet and visible light absorption spectra of syn-lutein epoxide (——), syn-neo-lutein epoxide A (A*) (----), syn-neo-lutein epoxide B (B*) (·····) (in HCl-benzene).

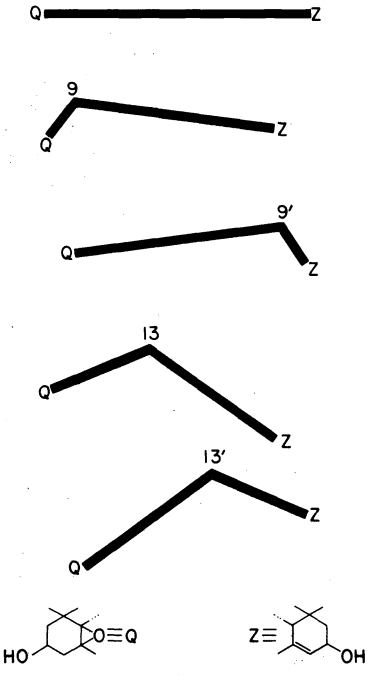


Fig. 25. Monocis lutein epoxides observed by iodine catalysis, in light.

Table 6. Composition of equilibrium mixtures of lutein epoxides isomerized by 120-min. refluxing of the benzene solution, in darkness

| Native (anti) lutein epoxide | | | | | | | |
|---|---|---|---|---|---|---|---|
| | Spectral data | | Relative E-values at 452 nm in % of the recovered pigments | | | | |
| Experiment | $\lambda_{max}$ shift nm | $E_{max}/E_{cis\text{-peak}}$ | Neo A + Neo A* | Neo B + Neo B* | Furanoids | Di-*cis* form | All-*trans* |
| 1. | 4 | 5.9 | 20.5 | | 4.7 | | 74.8 |
| 2. | 4 | 5.5 | 20.9 | | 3.1 | | 75.7 |
| 3. | 4 | 5.7 | 21.0 | | 3.2 | | 75.6 |
| | | Average value | 20.8 | | 3.3 | | 75.4 |
| Semisynthetic (syn) lutein epoxide | | | | | | | |
| 1. | 4 | 6.1 | 19.7 | | 2.3 | | 77.9 |
| 2. | 4 | 6.0 | 19.8 | | 3.1 | | 76.9 |
| 3. | 4 | 5.8 | 21.0 | | 2.4 | | 76.4 |
| | | Average value | 20.2 | | 2.6 | | 77.1 |

Table 7. Composition of equilibrium mixtures of lutein epoxides isomerized by iodine in light, for 30 min, at 24°C (in benzene)

| Native (anti) lutein epoxide | | | | | | | |
|---|---|---|---|---|---|---|---|
| | Spectral data | | Relative E-values at 452 nm in % of the recovered pigments | | | | |
| Experiment | $\lambda_{max}$ shift nm | $E_{max}/E_{cis\text{-peak}}$ | Neo A + Neo A* | Neo B + Neo B* | Furanoids | Di-*cis* | All-*trans* |
| 1. | 4 | 6.7 | 11.5 | 23.2 | 4.0 | 6.2 | 55.0 |
| 2. | 4 | 6.8 | 13.8 | 23.4 | 4.8 | 5.3 | 55.5 |
| 3. | 4 | 6.7 | 12.7 | 22.6 | 2.3 | 3.6 | 58.6 |
| | | Average value | 12.7 | 23.1 | 3.7 | 5.0 | 56.4 |
| Semisynthetic (syn) lutein epoxide | | | | | | | |
| 1. | 4 | 6.9 | 10.6 | 23.4 | | 6.5 | 60.0 |
| 2. | 4 | 6.8 | 12.7 | 22.9 | | 5.5 | 59.0 |
| 3. | 4 | 6.8 | 13.1 | 22.6 | | 6.1 | 58.4 |
| | | Average value | 12.1 | 23.0 | | 6.1 | 59.1 |

semisynthetic (syn) lutein epoxide[32] led to the discovery of four mono-*cis* isomers, too. Tables 6 and 7 show that stereomutation of native and semisynthetic lutein epoxide accomplished, either by refluxing or by iodine catalysis provides, in both cases, about the same equilibrium mixtures. In conclusion, differences at the chiral-centres did not influence the *cis–trans* isomerism connected with the polyene-chain.

This shows that, contrary to all previous suggestions, lutein epoxide has eight mono-*cis* isomers, namely four isomers in the native, and four in the semisynthetic series.

### AN ATTEMPT TO STUDY THE KINETICS OF *CIS–TRANS* ISOMERISATION

In spite of the detailed work already done in the field of *cis–trans* isomerism of carotenoids[1,3,33,34] no systematic study of the kinetics of this progress has previously been attempted. The reason is undoubtedly the complexity of the equilibrium mixtures and the lability of the isomers involved. It would, however, be well worth carrying out such investigations to clarify the mechanism of stereomutation.

When taking the first steps, we already had our doubts about the kinetic study of the stereomutation of carotenoids. Lutein epoxide was used as one of the simplest models for the illustration of a first order reversible reaction in carotenoid chemistry. According to our observations, all-*trans* lutein epoxide in benzene solution at elevated temperatures yields an equilibrium mixture in which only neolutein epoxide A (13- or 13′-*cis* form) appears. Furthermore, lutein epoxide when warmed in benzene solution and kept in the dark under dry nitrogen produces neither di-*cis*, nor furanoid derivatives.[35]

Considering that, in contrast to all-*trans* lutein epoxide, neolutein epoxide A exhibits a high *cis*-peak in the ultraviolet region, the changing ratio of the all-*trans* and neo A forms can be measured in time by spectroscopy as shown in Fig. 26. At the same time further information can be obtained about the isomerisation process by checking the extinction values at about 480–483 nm. After chromatographical separation, the above spectroscopial values were confirmed by quantitative analysis on several occasions.

Since the conversion was a first order reversible reaction, the rate law was easily integrated and the rate constants for the forward ($k$) and reverse ($k'$) directions calculated by equations[36] shown in Table 8. By substituting concentration for extinction values in the equations the calculation of rate constants (min) is simplified.

The results obtained in the present study can best be summed up by reviewing the Tables and Figures as follows:

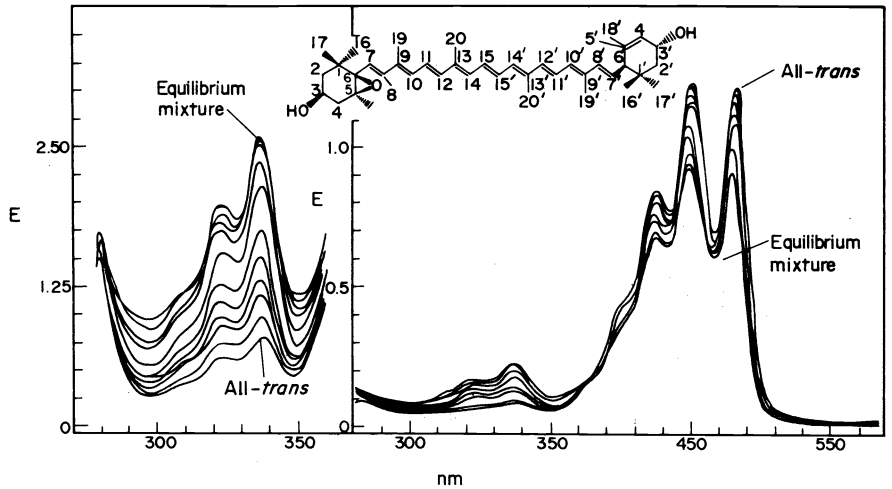


Fig. 26. Ultraviolet and light absorption spectra of syn (3S, 5S, 6R)-all-*trans*-lutein epoxide and mixture of the stereoisomers (all-*trans* + neo-A) after heat isomerization at 70°C, in darkness, for 0, 30, 70, 120, 200, 300, 480, 660, 900, 1140, 1260 min. (in benzene).

Table 8

$$2\ \text{Lutein epoxide} \underset{k'}{\overset{k}{\rightleftharpoons}} \text{Neolutein epoxide A} + \text{Neolutein epoxide A}^*$$

$$[\text{Neolutein epoxide A}] \cong [\text{Neolutein epoxide A}^*]$$

$$\text{Lutein epoxide} \underset{K'}{\overset{k}{\rightleftharpoons}} \text{NEOLUTEIN EPOXIDE A}$$

$$\ln \frac{[\text{Lutein epoxide}]_0 - [\text{Lutein exoxide}]_e}{[\text{Lutein epoxide}] - [\text{Lutein epoxide}]_e} = (k + k')t$$

$$\frac{k + k'}{[\text{Lutein epoxide}]_0} [\text{Lutein epoxide}]_e = k'$$

Where the subscript e refers to equilibrium concentration and the subscript 0 to concentration at 0 time.

Table 9. Ratio of E-values in the equilibrium mixtures of all-*trans* lutein epoxide and neolutein epoxide A at 60–75°

| | Starting material | | | | | | |
|---|---|---|---|---|---|---|---|
| | All-*trans* lutein epoxide | | | Neolutein epoxide A | | | |
| Temperature °C | 60 | 65 | 75 | 60 | 65 | 70 | 75 |
| $E_{cis}/E_{trans}$ at 337 nm | 3.08 | 2.92 | 3.09 | 3.18 | 3.00 | 2.91 | 3.08 |
| Average value | | 3.03 | | | 3.04 | | |

(a) Table 9 shows that the extinction ratios of the neo A and all-*trans* forms are constant in the equilibrium mixtures. The ratio is independent of the direction of the stereomutation, i.e. it makes no difference whether it is started from the all-*trans*, or the neo A form.

(b) The ratio does not depend on temperature between 60° and 75°C, within experimental errors (see Table 9).

(c) Figure 27 demonstrates the change of extinction values for neo A in time at various temperatures. Normally, the rate of isomerisation of the all-*trans* form increases with rising temperature. Figure 28 shows the same experiments with the neo A form; the rate of formation of all-*trans* lutein epoxide increases with rising temperature.

(d) Tables 10 and 11 give some information on rate constants, which usually decrease with time. In fact, the *cis–trans* conversion has a fast phase at the beginning. We calculated the *k*-values for the faster phase, and simply use of their arithmatical mean. Tables 10 and 11 show the lack of necessary coincidence of the rate constants when the rate constants calculated from the forward and reverse directions are compared.

(e) The Arrhenius-time curve in Fig. 29 demonstrates that the log *k*-values coincide reasonably well. The energy of activation calculated graphically is 28 Kcal. (Because of the error in the calculation of rate constants, the same error, was of course, obtained by the calculation of Ea.)

Finally, it should be emphasised that this investigation into the kinetics of *cis–trans* isomerization in the field of

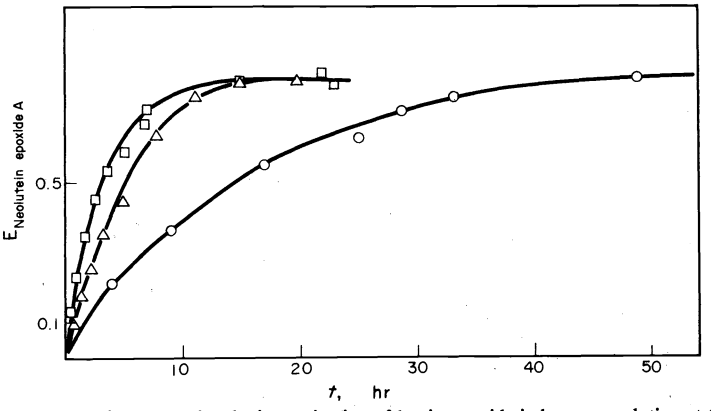


Fig. 27. Concentration (E)-time curve for the isomerization of lutein epoxide in benzene solution at 60–75°, in dark (○—○ 60.3°C; △—△ 70.2°C; □—□ 75.2°C).

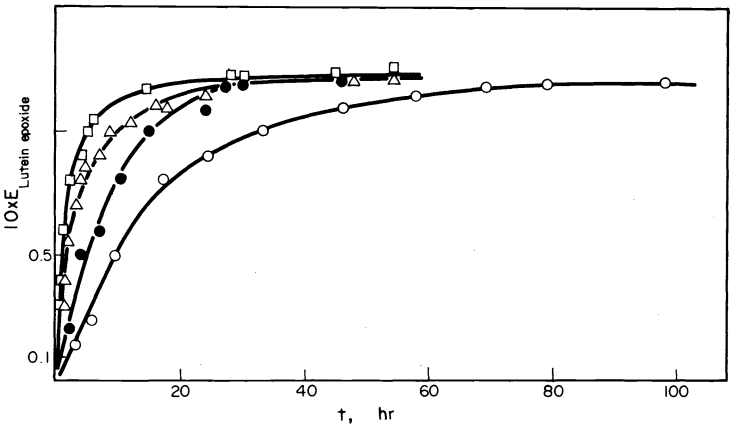


Fig. 28. Concentration (E)-time curve for the isomerization of neolutein epoxide A in benzene solution at 60–75°, in dark (○—○ 60.3°C, ●—■ 65.0°C; △—△ 70.2°C; □—□ 75.2°C).

Table 10. Influence of temperature on the rate constants.† ([Lutein epoxide]$_0$ = $1.7 \times 10^{-4}$ M; incubated in benzene solution at darkness and protected from air)

Lutein epoxide $\underset{k'}{\overset{k}{\rightleftharpoons}}$ Neolutein epoxide A

| 60.3°C | | 70.2°C | | 75.2°C | |
|---|---|---|---|---|---|
| $k$ | $k'$ | $k$ | $k'$ | $k$ | $k'$ |
| $3.60 \cdot 10^{-4}$ | $7.80 \cdot 10^{-4}$ | $1.54 \cdot 10^{-3}$ | $2.77 \cdot 10^{-3}$ | $1.82 \cdot 10^{-3}$ | $3.97 \cdot 10^{-3}$ |
| $3.42 \cdot 10^{-4}$ | $7.42 \cdot 10^{-4}$ | $1.42 \cdot 10^{-3}$ | $2.55 \cdot 10^{-3}$ | $1.76 \cdot 10^{-3}$ | $3.84 \cdot 10^{-3}$ |
| $3.38 \cdot 10^{-4}$ | $7.32 \cdot 10^{-4}$ | $1.39 \cdot 10^{-3}$ | $2.51 \cdot 10^{-3}$ | $1.71 \cdot 10^{-3}$ | $3.73 \cdot 10^{-3}$ |
| $3.18 \cdot 10^{-4}$ | $7.02 \cdot 10^{-4}$ | $1.16 \cdot 10^{-3}$ | $2.08 \cdot 10^{-3}$ | $1.69 \cdot 10^{-3}$ | $3.69 \cdot 10^{-3}$ |
| $3.39 \cdot 10^{-4}$ | $7.39 \cdot 10^{-4}$ | $1.37 \cdot 10^{-3}$ | $2{,}48 \cdot 10^{-3}$ | $1.75 \cdot 10^{-3}$ | $3.81 \cdot 10^{-3}$ |

†These data refer to the faster phase of the rearrangement; $k(k')\ \text{min}^{-1}$.

Table 11. Influence of temperature on the rate constants.† ([Neolutein epoxide A]$_0 \sim 1.7 \times 10^{-4}$ M; incubated in benzene solution at darkness and protected from air)

Neolutein epoxide A $\underset{k}{\overset{k'}{\rightleftharpoons}}$ Lutein epoxide

| 60.3°C | | 65.0°C | | 70.2°C | | 75.2°C | |
|---|---|---|---|---|---|---|---|
| $k$ | $k'$ | $k$ | $k'$ | $k$ | $k'$ | $k$ | $k'$ |
| $3.12 \cdot 10^{-4}$ | $6.43 \cdot 10^{-4}$ | $0.53 \cdot 10^{-3}$ | $1.06 \cdot 10^{-3}$ | $1.35 \cdot 10^{-3}$ | $3.04 \cdot 10^{-3}$ | $2.49 \cdot 10^{-3}$ | $4.37 \cdot 10^{-3}$ |
| $3.19 \cdot 10^{-4}$ | $6.59 \cdot 10^{-4}$ | $0.63 \cdot 10^{-3}$ | $1.25 \cdot 10^{-3}$ | $1.11 \cdot 10^{-3}$ | $2.49 \cdot 10^{-3}$ | $2.14 \cdot 10^{-3}$ | $4.04 \cdot 10^{-3}$ |
| $3.54 \cdot 10^{-4}$ | $7.31 \cdot 10^{-4}$ | $0.59 \cdot 10^{-3}$ | $1.17 \cdot 10^{-3}$ | $1.01 \cdot 10^{-3}$ | $2.25 \cdot 10^{-3}$ | $2.27 \cdot 10^{-3}$ | $4.29 \cdot 10^{-3}$ |
| $3.14 \cdot 10^{-4}$ | $6.47 \cdot 10^{-4}$ | $0.55 \cdot 10^{-3}$ | $1.09 \cdot 10^{-3}$ | $0.95 \cdot 10^{-3}$ | $2.12 \cdot 10^{-3}$ | $1.87 \cdot 10^{-3}$ | $3.53 \cdot 10^{-3}$ |
| $3.25 \cdot 10^{-4}$ | $6.70 \cdot 10^{-4}$ | $0.57 \cdot 10^{-3}$ | $1.14 \cdot 10^{-3}$ | $1.10 \cdot 10^{-3}$ | $2.47 \cdot 10^{-3}$ | $2.19 \cdot 10^{-3}$ | $4.06 \cdot 10^{-3}$ |

†These data refer to the faster phase of the rearrangement; $k(k')\ \text{min}^{-1}$.

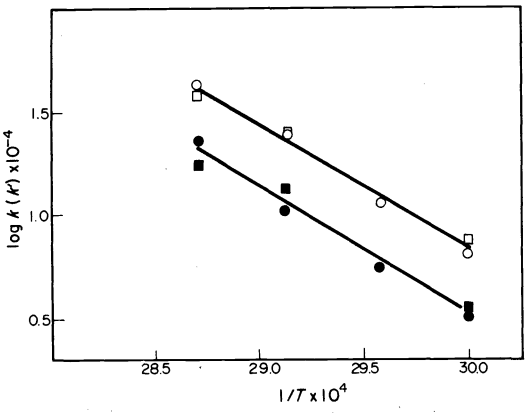


Fig. 29. Arrhenius temperature dependence of the rate constants: $k$, $k'$; Calculated for ○, □; Neolutein epoxide A ⇌ Lutein epoxide: ●, ■; Lutein epoxide ⇌ Neolutein epoxide A.

carotenoids represents only a rough approximation to the problem and an early search for ways of further investigation.

*Acknowledgements*—I warmly thank my collaborators, in particular M. Baranyai (capsanthin set, lutein epoxide set, neocapsorubin A, neocapsorubin B), P. Molnár (controlled oxidative degradation, kinetic study) and Dr. Gy. Tóth (neozeaxanthin A, neozeaxanthin B), who have done most of the work in the present paper.

I also wish to emphasize the excellent contribution of Dr. Radics (Central Research Institute for Chemistry, Budapest), upon whose work on carbon-13 nuclear magnetic resonance a chapter of this lecture is based.

## REFERENCES

[1]L. Zechmeister, Cis–Trans *Isomeric Carotenoids, Vitamins A and Arylpolyenes.* Springer, Vienna (1962).
[2]H. Mayer and O. Isler, *Carotenoids* (editor O. Isler), Chap. 6. Birkhäuser, Basle (1971).
[3]B. C. L. Weedon, *Carotenoids* (editor O. Isler), Chap. 5. Birkhäuser, Basle (1971).
[4]U. Schwieter, G. Englert, N. Rigassi and W. Vetter, *Pure Appl. Chem.* **20**, 365 (1969).
[5]J. B. Stothers, *Carbon-13 NMR Spectroscopy.* Academic Press, London (1972).
[6]R. Rowan, III and B. D. Sykes, *J. Am. chem. Soc.* **96**, 7000 (1974).
[7]R. S. Becker, S. Berger, Don K. Dalling, D. M. Grant and R. J. Pugmire, *J. Am. chem. Soc.* **96**, 7008 (1974).
[8]P. Molnár and J. Szabolcs, *Acta Chim. Acad. Sci. Hung.* **79**, 465 (1973)
[9]P. Karrer and U. Solmssen, *Helv. Chim. Acta*, **20**, 682 (1937).
[10]P. Karrer, U. Solmssen and W. Gugelmann, *Helv. Chim. Acta*, **20**, 1020 (1937).
[11]P. Karrer, A. Rüegger and A. Geiger, *Helv. Chim. Acta*, **21**, 1171 (1938).
[12]H. H. Strain, *Arch. Biochem. Biophys.* **48**, 458 (1954).
[13]J. Szabolcs and Gy. Tóth, *Acta Chim. Acad. Sci. Hung.* **63**, 229 (1970).
[14]G. P. Moss, J. Szabolcs, Gy. Tóth and B. C. L. Weedon, *Acta Chim. Acad. Sci. Hung.* In press.
[15]L. Cholnoky, K. Györgyfy, A. Rónai, J. Szabolcs and Gy. Tóth, Gail Galasko, A. K. Mallams, E. S. Waight and B. C. L. Weedon, *J. Chem. Soc. C*, 1256 (1969).
[16]A. K. Mallams, E. S. Waight, B. C. L. Weedon, L. Cholnoky, K. Györgyfy, J. Szabolcs, N. I. Krinsky, B. P. Schimmer, C. O. Chichester, T. Katayama, L. Lowry and H. Yokoyama, *Chem. Commun.* 484 (1967).
[17]A. L. Curl, *J. Food Sci.* **32**, 141 (1967).
[18]L. Zechmeister and A. Polgár, *J. Am. Chem. Soc.* **66**, 137 (1944).
[19]W. Bremser and J. Paust, *Org. Magn. Res.*, **6**, 433 (1974).
[20]L. Zechmeister and R. M. Lemmon, *J. Am. chem. Soc.* **66**, 317 (1944).
[21]L. Zechmeister and L. Cholnoky, *Liebigs Ann. Chem.* **530**, 291 (1937).
[22]P. Pauling, *Helv. Chem. Acta*, **32**, 2241 (1949).
[23]H. H. Inhoffen, F. Bohlmann and G. Rummert, *Liebigs Ann. Chem.* **571**, 75 (1951).
[24]L. Zechmeister and L. Cholnoky, *Liebigs Ann. Chem.* **543**, 248 (1940).
[25]A. Polgár and L. Zechmeister, *J. Am. Chem. Soc.* **66**, 186 (1944).
[26]A. J. Aasen, G. W. Francis and S. Liaaen-Jensen, *Acta Chem. Scand.* **23**, 2605 (1969).
[27]J. Szabolcs and Gy. Tóth, *Acta Chim. Acad. Sci. Hung.* **63**, 229 (1970).
[28]G. F. Crozier, *Biochem. Physol.* **23**, 179 (1967).
[29]H. Kleinig and H. Nietsche, *Phytochem.* **7**, 1171 (1968).
[30]K. Egger, *Planta*, **80**, 65 (1968).
[31]Gy. Tóth and J. Szabolcs, *Acta Chim. Acad. Sci. Hung.* **64**, 393 (1970).
[32]L. Bartlett, W. Klyne, W. P. Mose and P. M. Scopes, P. Galasko, A. K. Mallams and B. C. L. Weedon, J. Szabolcs and Gy. Tóth, *J. Chem. Soc. C*, **2527** (1969).
[33]A. Pulmann and B. Pullmann, *Proc. Nat. Acad. Sci. USA*, **47**, 7 (1961).
[34]P. Pauling, *Fortschr. Chem. Org. Naturst.* **3**, 203 (1939).
[35]Kerényi Lászlóné és Szabolcs József, *Magyar Kém. Folyóirat*, **78**, 122 (1972).
[36]A. A. Frost and R. G. Pearson, *Kinetics and Mechanism.* p. 152. J. Wiley, New York (1953).